Available online at www.sciencedirect.com
ScienceDirect
Postharvest Biology and Technology 41 (2006) 285–295
Postharvest Biology and Technology
www.elsevier.com/locate/postharvbio

Calibrated color measurements of agricultural foods using image analysis

Fernando Mendoza [a,*], Petr Dejmek [b], José M. Aguilera [a]

[a] *Department of Chemical Engineering and Bioprocess, Pontificia Universidad Católica de Chile, P.O. Box 306, Santiago, Chile*
[b] *Department of Food Engineering, Chemical Center, Lund University, P.O. Box 124, 221 00 Lund, Sweden*

Received 24 August 2005; accepted 8 April 2006

Abstract

A computer vision system (CVS) was implemented to quantify standard color of fruit and vegetables in *sRGB*, *HSV* and $L^*a^*b^*$ color spaces, and image capture conditions affecting the results were evaluated. These three color spaces are compared in terms of their suitability for color quantification in curved surfaces. The results show that *sRGB* standard (linear signals) was efficient to define the mapping between $R'G'B'$ (no-linear signals) from the CCD camera and a device-independent system such as CIE *XYZ*. The CVS showed to be robust to changes in sample orientation, resolution, and zoom. However, the measured average color was shown to be significantly affected by the properties of the background and by the surface curvature and gloss. Thus all average color results should be interpreted with caution. $L^*a^*b^*$ system is suggested as the best color space for quantification in foods with curved surfaces.

Keywords: *sRGB* standard; CIE color; Computer vision sensitivity; Curved surfaces

1. Introduction

Color is considered a fundamental physical property of agriculture products and foods, since it has been widely demonstrated that it correlates well with other physical, chemical and sensorial indicators of product quality. In fact, color plays a major role in the assessment of external quality in food industries and food engineering research (Segnini et al., 1999; Abdullah et al., 2001).

Color can be rapidly analyzed by computerized image analysis techniques, also known as computer vision systems (CVS). These systems not only offer a methodology for measurement of uneven coloration but it can also be applied to the measurement of other attributes of total appearance (Hutchings, 1999). So far it has not been attempted in the published literature to detect all the optical properties of an object from object images, and in particular, for those with irregular surfaces. However, calibrated average color measurements and other appearance features using computer vision techniques have been shown to closely correlate with those from the visual assessment (Mendoza and Aguilera, 2004).

Dedicated commercial vision systems are currently available for a variety of industrial applications, and they are especially recommended for color assessments in samples with curved and irregular shapes of the surface; however, the effects of these physical properties and how they are handled to give representative measurements is frequently not known. The knowledge of these effects, such as the variations of L^*, a^*, and b^* for a particular shape of the sample, could be useful for developing image processing correction algorithms which can permit a better correlation among product quality by CVS and human vision evaluations.

The objectives of this study were: (i) to implement a computerized image analysis technique to quantify standard color according to the CIE system based on the *sRGB* standard; (ii) to assess the effect of changes in the commonly used capture conditions of the CVS with regard to the initial calibration conditions using $L^*a^*b^*$ color space; and (iii) to critically assess the sensitivity of the *RGB*, $L^*a^*b^*$ and *HSV* color spaces to represent the color in curved surfaces such as bananas and red pepper.

* Corresponding author. Tel.: +56 2 354 4254; fax: +56 2 354 5803.
E-mail address: fmendoza@ing.puc.cl (F. Mendoza).

0925-5214/$ – see front matter © 2006 Elsevier B.V. All rights reserved.
doi:10.1016/j.postharvbio.2006.04.004

2. Materials and methods

2.1. Color concepts

Color is basically specified by the geometry and spectral distributions of three elements: the light source, the reflectivity of the sample and the visual sensitivity of observer. Each of these was defined by the *Commission Internationale de l'Eclairage* (CIE) in 1931. The definition was aimed at simulating the human color perception based on a 2° field of view, a set of primaries (red, green, blue), and color-matching functions (CIE, 1986). The matching functions for the *standard observer* ($\bar{x}$, $\bar{y}$, $\bar{z}$) are defined so that the individual spectra of primaries can be used to compute the perceived brightness or luminance of a measured color according to Grassman's additive law, and using an artificial triplet of 'primary lights' *X*, *Y* and *Z*. Thus, any color can be described by a combination of these primaries. By definition, *X*, *Y*, *Z* specifications of objects are always made relative to the luminosity of a perfect white object (reflectance equal to 100 at each wavelength). The *Y* for the perfect white is always 100. The magnitudes of *X* and *Z* for the perfect white change with the color of the illuminant being used (Hunter and Harold, 1987).

The human vision has three sets of sensors with peak sensitivities at light frequencies of 580 nm for red, 540 nm for green, and 450 nm for blue. Light at any wavelength in the visual spectrum range from 400 to 700 nm will excite one or more of these three types of sensors. Our perception of which color we are seeing is determined by which combination of sensors are excited and by how much. However, the observed light intensity of a given object depends on both the intensity and the spectral distribution of the illuminating light, and the spectral distribution of the object reflectivity. Consequently, CIE also defined spectral properties of several *standard illuminants* which are specified by their color temperatures. The most common one is standard illuminant D_{65}, corresponding to the radiation of a black body at 6500 K, which is intended to represent average daylight (Hunt, 1991). Later, in 1976 CIE specified two color spaces characterized as being less illumination-dependent, namely, the commonly used $L^*a^*b^*$ or CIELAB and $L^*u^*v^*$ or CIELUV (Robertson, 1976). L^*, a^*, and b^* values are calculated from *XYZ* values of a colored object under a given illuminant and *XYZ* values of a reference white object under the same illuminant.

In the assessment of food color, the advent of new laboratory instruments in recent years mean that measurements which were previously only plausible via human senses, can now readily be made instrumentally. Conventional color specification instruments (such as colorimeters and spectrophotometers) are one of the instrumental tools which usually provide readings in *XYZ*, *RGB* and $L^*a^*b^*$ color space. Tristimulus colorimeters use filters in combination with a light source and detector to spectrally emulate the standard observer functions of the eye, given direct evaluations of *X*, *Y*, and *Z*. Spectrophotometers give wavelength-by-wavelength analyses of the light reflecting or light transmitting properties of objects throughout the visible range. The areas under the resulting curves can be converted into *X*, *Y*, and *Z* (Hunter and Harold, 1987). Although these instruments are suitable for use with food materials, they are inherently unsuitable for assessing the color distribution and color uniformity measurements of many whole foods (Hutchings et al., 2002). These instruments only provide average values of small areas of the sample, and therefore, many locations must be measured to obtain a representative color profile.

Alternatively, CVSs used for color measurements were developed in response to the low spatial resolution of the conventional instrumental techniques. The advantages with respect to the traditional techniques have been illustrated in many investigations (Shahin and Symons, 2001; Chen et al., 2002; O'Sullivan et al., 2003; Brosnan and Sun, 2002, 2004; Yam and Papadakis, 2004; Du and Sun, 2004). Basically, a CVS consists of a digital or video camera for image acquisition, standard illuminants, and a computer software for image analysis (Papadakis et al., 2000; Brosnan and Sun, 2004).

Digital and video cameras are powerful tools for image acquisition and color studies. However, there are some issues that are important to consider for high-fidelity cross-media color reproduction and color measurements. The majority of color digital still cameras being used for technical applications employ a single array of light-sensitive elements on a CCD chip, with a filter array that allows some elements to see red (*R*), some green (*G*) and some blue (*B*) and, whose relative intensities could be manually or automatically adjusted by a function called 'white balance'. Such cameras devote half of the elements to green sensitivity, and one quarter each to red and blue, emulating human vision which is most sensitive in the green portion of the spectrum. Thus, a digital color image is represented in *RGB* form with three components per pixel in the range 0–255 and conventionally stored using eight bits per color component. These three intensity images (*R*, *G* and *B*) are thus electronically combined to produce a digital color picture (Russ, 2005).

Consequently, it is obvious that *RGB* signals generated by a CCD are device-dependent, i.e. each camera has its own different color sensor characteristics and produce different *RGB* responses for the same image when it is displayed through graphic card of a standard monitor (Segnini et al., 1999; Hutchings et al., 2002). For grayscale imaging this may not be too serious, but for color it can be, especially where colorimetric precision is important. Moreover, contributing to disagreement is the fact that the CCD response characteristics are not identical to the CIE color-matching functions, since the CCD sensors do not have the same spectral sensitivities or gamut of colors as the CIE standard observer.

Another important issue to consider in color reproduction and color measurements is *gamma*. Cathode-ray tube (CRT) displays, as used in computer monitors and television sets, are inherently nonlinear; meaning that the intensity of light reproduced at the screen of a CRT display is not proportional to its voltage input. To achieve adequate performance with eight bits per color component these CRT displays require nonlin-

ear coding (Poynton, 1996). The nonlinearity of a CRT is very nearly the inverse of the lightness sensitivity of human vision, and consequently, the image display on a standard computer monitor is appreciated as the original image. In addition, the balance of power in CRTs among the three electron beams – the white point – determines the color assigned to white. These parameters are different for different monitors, and color reproduction is not predictable without control of these parameters (Sangwine, 2000). In practice, this nonlinearity is usually corrected for in the conversion algorithm by a power law correction, which exponent is called *gamma* and usually has values in the range of 2.3–2.6 (Poynton, 1996). The vast majority of computer monitors in use today were shown to have the average CRT gamma 2.2 with a standard deviation of about 0.2, when the black level offset and the gain of the CRT were optimally set (Stokes et al., 1996). CRT hardware will thus automatically decode image pixels that have been encoded by raising them to the power 1/2.2. This property is exploited in video encoding systems.

In order to measure an object in terms of device-independent color from a digital camera and CRT display, there is a need to correlate the camera $R'G'B'$ signals and CIE *XYZ* tristimulus values. That is to say, using a power function with a suitable gamma value which is applied to each R', G', B' signal. This is known as camera characterization. The most common technique for digital camera characterization consists of presenting the camera with a series of color patches in a standardized reference chart with known *XYZ* values and recording the averaged *RGB* signals for each patch. Polynomial fitting techniques can then be applied to interpolate the data over the full range and to generate inverse transformations (Hutchings et al., 2002). However, the basic problem is how to produce an image that is in some sense equivalent to the original on different devices without needing to define separate transformation for each pair of light source and target device, and whose color information can be easily transferable and reproduced between different laboratories or industries on the basis of a common interchange format.

sRGB (Standard *RGB*) is an international color standard defined by the *International Electrotechnical Commission* (IEC) as IEC 61966-2-1 (1999). The standard defines a virtual display based on a typical CRT color gamut including phosphor characteristics, a white point and the maximum luminance of the display, and a single linear transformation which defines approximately the mapping between $R'G'B'$ signals from the CDC and a device-independent system such as CIE *XYZ* (Stokes et al., 1996). The use of the color space *sRGB* is consistent with but is a more tightly defined derivative of Rec. ITU-R BT.709-5 (2002) as the standard color space for the operative systems and the Internet. The ITU-R BT.709 recommendation specifically describes the encoding transfer function for a video camera that when viewed on a "standard" monitor will produce excellent image quality. *sRGB* has been adopted by a wide range of applications, including Adobe Photoshop, JASC Paintshop, and is the default color space for Microsoft Windows color management and for many desktop printers (Gondek, 2000). Modern digital cameras are designed to deliver images congruent to *sRGB* standard.

2.2. Color measurements

2.2.1. Fruit samples

Eight bananas (cv *Musa cavendish*) at the ripening stages 1 (green), 6 (all yellow), and 7 (yellow, flecked with brown) and one red pepper (cv *Capsicum frutescens*) with only slight defects were selected from a commercial distributor in Sweden.

2.2.2. Conventional colorimeter

A colorimeter, Dr. Lange Micro Colour (Dr. Lange, Germany), was used as standard color for the calibration of the computer vision system since this instrument readout can be set to any CIE units. Its technical characteristics are: 10° for the normal observer, D65 as the standard illuminant, and a measuring surface of 5 mm^2. The white reference used was according to DIN 5033 (white reference model Weiβ-Standard LZM 076, Dr. Lange, Germany), and its reference values were $Xn = 78.2$, $Yn = 83.1$, and $Zn = 89.9$.

2.2.3. Computer vision system (CVS)

The CVS consisted of the following elements.

2.2.3.1. Lighting system. Samples were illuminated using two parallel lamps (with two fluorescents tubes in each lamp, TL-D Deluxe, Natural Daylight, 18W/965, Philips, USA) with a color temperature of 6500 K (D_{65}, standard light source commonly used in food research) and a color-rendering index (R_a) close to 95%. Both lamps (60 cm long) were situated 35 cm above the sample and at an angle of 45° to the sample. Additionally, light diffusers covering each lamp and electronic ballast assured a uniform illumination system.

2.2.3.2. Digital camera and image acquisition. A Color Digital Camera (CDC), model PowerShot A70 (Canon, USA) was located vertically over the background at a distance of 30 cm. The angle between the camera lens and the lighting source axis was approximately 45°, since the diffuse reflections responsible for the color occurs mainly at this angle from the incident light (Francis and Clydesdale, 1975). Also, considering that ambient illumination is critical for reproducible imaging (Shahin and Symons, 2001), sample illuminators and the CDC were covered with a black cloth to avoid the external light and reflections. As standard capture conditions, images were taken on a matte black background and using the following camera settings: manual mode with the lens aperture at $f = 4.5$ and speed 1/125, no zoom, no flash, intermediate resolution of the CDC (1024 × 768) pixels, and storage in JPEG format. The white balance of the camera was set using the same white reference as the colorimeter. The camera was connected to the USB port of a PC provided with a Remote Capture Software (Version 2.7.0, Canon, USA) to

visualize and acquire the digitalized images directly from the computer.

2.2.3.3. Image processing. All the algorithms for preprocessing of full images, segmentation from the background, and color analysis were written in MATLAB 6.5 (The MathWorks, Inc., USA).

2.2.4. Calibration of the CVS

The standard *sRGB* (IEC 61966-2-1, 1999) involves two parts: (i) the viewing environment parameters, which are recommended for viewing photographic images on monitors; and (ii) the definitions and transformations standard device space colorimetric which provide the necessary transforms to convert between the *sRGB* color space and the CIE *XYZ* color space (Stokes et al., 1996). Thus, *sRGB* in combination with the reference viewing environments can be defined from non-uniform encoding mapping functions that is applied to all three primaries (R', G', B') obtained from a specific capture device in the theoretical range of 0–255.

In this context, for the characterization of the CCD and transformation of computer $R'G'B'$ into CIE space, 125 color sheets with different hues (from red to violet) including white and black sheets from Pantone® Colour Formula Guide (Pantone, Inc., USA) were photographed and analyzed using the CVS to obtain the $R'G'B'$ values. Similarly, *RGB* and *XYZ* values of each color sheet were measured by a conventional colorimeter (Dr. Lange, Germany) in three equidistant points. The comparison of color results between CVS and conventional colorimeter using the same white reference allowed characterisation of the CCD and confirmation of the suitability of the standard *sRGB* for calibration of this particular image acquisition system. IEC 61966-2-1 (1999) defines the transformation from floating point nonlinear $R'G'B'$ values to CIE *XYZ* in two steps:

(1) The nonlinear $R'G'B'$ values are transformed to linear *sRGB* values by

If $R', G', B' \leq 0.04045$

$$sR = \frac{R'}{12.92}, \quad sG = \frac{G'}{12.92}, \quad sB = \frac{B'}{12.92} \tag{1}$$

else if $R', G', B' > 0.04045$

$$sR = -\left(\frac{-R' + 0.055}{1.055}\right)^{2.4},$$

$$sG = -\left(\frac{-G' + 0.055}{1.055}\right)^{2.4},$$

$$sB = -\left(\frac{-B' + 0.055}{1.055}\right)^{2.4} \tag{2}$$

(2) Then, using the recommended coefficients by the Rec. ITU-R BT.709-5 (2002), *sRGB* values are converted to the CIE *XYZ* system by

$$\begin{bmatrix} X \\ Y \\ Z \end{bmatrix} = \begin{bmatrix} 0.4124 & 0.3576 & 0.1805 \\ 0.2126 & 0.7152 & 0.0722 \\ 0.0193 & 0.1192 & 0.9505 \end{bmatrix} \begin{bmatrix} sR \\ sG \\ sB \end{bmatrix} \tag{3}$$

In the $R'G'B'$ encoding process, the power function with a gamma factor of 2.4 includes a slight black-level offset to allow for invertability in integer math which closely fit a straightforward gamma 2.2 curve (Stokes et al., 1996). Therefore, consistency was maintained with the gamma 2.2 legacy images and the video industry. Also, *sRGB* tristimulus values less than 0.0 or greater than 1.0 were clipped to 0.0 and 1.0, respectively, since this gamut is large enough to encompass most colors that can be displayed on CRT monitors.

2.2.5. Image segmentation

Background was removed from the preprocessed gray scale image using a threshold of 50 combined with an edge detection technique based on the Laplacian-of-Gauss (LoG) operator (Castleman, 1996). The gray scale image was obtained using the function *'rgb2gray'* of Matlab. The LoG-operator involved a Gaussian lowpass filter with mask size [3 3] and sigma 0.5, which permits pre-smoothing of noisy images. This segmented image is a binary image, where '0' (black) and '1' (white) mean background and object, respectively. So, from this binary image, the localization of the pixels into the interest region permitted us to extract from the original image the true color image of the sample.

2.2.6. Color spaces

In food research, color is frequently represented using the $L^*a^*b^*$ color space. This color model is considered approximately uniform, i.e. distance between two colors in a linear color space corresponds to the perceived differences between them. Therefore, it permits an objective color representation and its use is essential for applications where the results must match those of the human perception (Sangwine, 2000). L^* is the luminance or lightness component that goes from 0 (black) to 100 (white), and parameters a^* (from green to red) and b^* (from blue to yellow) are the two chromatic components, varying from −120 to +120. The definition of $L^*a^*b^*$ is based on the intermediate system CIE *XYZ* which simulates the human perception (Rec. ITU-R BT. 709-5, 2002) and which may be converted from *RGB*, as showed in Eq. (3). Thus, L^*, a^*, and b^* are defined as

$$L^* = 116 f\left(\frac{Y}{Yn}\right) - 16 \tag{4}$$

$$a^* = 500\left[f\left(\frac{X}{Xn}\right) - f\left(\frac{Y}{Yn}\right)\right] \tag{5}$$

$$b^* = 200\left[f\left(\frac{Y}{Yn}\right) - f\left(\frac{Z}{Zn}\right)\right] \tag{6}$$

where

$$f(q) = \begin{cases} q^{1/3} & \text{if } q > 0.008856 \\ 7.787q + 16/116 & \text{otherwise} \end{cases} \quad (7)$$

Xn, *Yn*, and *Zn* correspond to the *XYZ* values of a reference white chart ($q \in \{X/Xn, Y/Yn, Z/Zn\}$).

The total color difference between two colors in L^*, a^* and b^* coordinates may be evaluated as

$$\Delta E^*_{ab} = [(\Delta L^*)^2 + (\Delta a^*)^2 + (\Delta b^*)^2]^{1/2} \quad (8)$$

A less used color space in foods is the *HSV*. It is a user-oriented color system based on the artist's idea of tint, shade and tone. *HSV* separates color into three components varying from 0 to 1 (when it is calculated using the function *rgb2hsv* available in Matlab®); *H* (hue) refers to the dominant wavelength perceived as different colors, such as red, yellow, green and blue, *S* (saturation) refers to how much such wavelength is concentrated and it is equivalent to the concentration of a solute in a chemical solution; and *V* (value) represents the total brightness, similar to L^*. The computation of *H*, *S*, and *V* values considers the transformation from *RGB* to *HSV* color space according to the following expressions (Du and Sun, 2005):

$$V = \max(R, G, B) \quad (9)$$

$$S = \frac{V - \min(R, G, B)}{V} \quad (10)$$

$$H = \begin{cases} 1 + \dfrac{G - B}{V - \min(R, G, B)} & \text{for } V = R \\ 3 + \dfrac{B - R}{V - \min(R, G, B)} & \text{for } V = G \\ 5 + \dfrac{R - G}{V - \min(R, G, B)} & \text{for } V = B \end{cases} \quad (11)$$

After segmentation of the image and transformation of computer R', G', and B' into CIE space, the color data were converted to $L^*a^*b^*$ and *HSV* color spaces. The average value of the pixels for each color scale in the segmented image was registered as the color of the samples.

2.2.7. Sensitivity analysis of CVS color measurements

For an objective color reproduction and comparison among samples, it is advisable and desirable that the setting capture conditions of the CVS are the same as those used for the calibration process. However, some setting conditions may require changes for particular products, namely: (i) color of the background, enhancing the color contrast between the sample and background facilitating the image segmentation process; (ii) orientation of the sample on the background, which could affect the light reflections, particularly, in samples with curved surfaces; (iii) resolution of the CCD, using a lower quality (640 × 480) to diminish the processing time of complex images; and (iv) zoom of the lens, which is usually needed so that the smaller samples fulfill the whole field of view.

In order to assess the color sensitivity of the CVS in relation to the changes in the image capture conditions and the variations of light reflections on curved surfaces, two experiments were carried out. In the first experiment, the effect of: the color of the background (black and white), sample orientation (0°: horizontal and 90°: vertical), resolution of the CCD (640 × 480 and 2048 × 1536 pixels), and zoom (focal length, 5.4 and 11.3 mm) on color measurements within the $L^*a^*b^*$ color system was computed for six bananas in ripening stage 7 (yellow, flecked with brown). For that a two-level full factorial 2^4 design was used which involves all possible combinations of factor modalities (see Table 1). The modalities for each factor were chosen according to the best capture conditions range which could allow well defined images of varied sizes of fruits and vegetables. In this particular experiment, to allow a focal length of 11.3 mm (high level), so that the full image of the banana was covered in the field of view, the CCD was located 40 cm above the background. Analysis of variance and Pareto charts of effects were used to define the most important factors and their interactions affecting the L^*, a^*, and b^* color measurements in bananas.

In a second experiment, the effect on the color measurements of *sRGB*, *HSV* and $L^*a^*b^*$ color spaces were analyzed and compared in relation to the suitability to represent color in curved surfaces. For that purpose images of a single yellow sheet (with homogeneous color) flat or rolled into a cylinder of 3.6 cm diameter was used (Fig. 1a and b). The *sRGB* and $L^*a^*b^*$ scales were normalized between 0 and 1 to facilitate comparison. The normalized values for *sR*, *sG* and *sB* were obtained by dividing the value of each pixel by 255 and for L^*, a^*, and b^* using the following equations (Papadakis et al., 2000):

$$\text{normalized } L^* = \frac{L^*}{100} \quad (12)$$

$$\text{normalized } a^* = \frac{a^* + 120}{240} \quad (13)$$

$$\text{normalized } b^* = \frac{b^* + 120}{240} \quad (14)$$

The images of bananas (green and yellow) and a red pepper were tested. These foods were selected since they present very homogeneous peel color in these ripening stages and have a characteristic waved surface (see Fig. 1c and e).

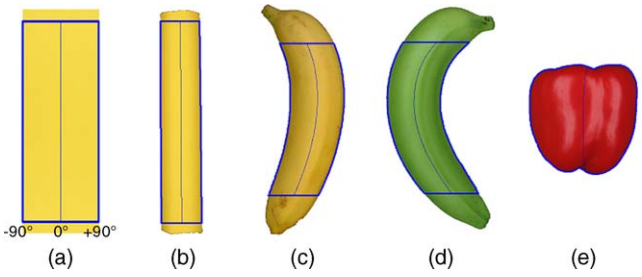

Fig. 1. Segmented regions used in the color profile analysis: (a) flat yellow sheet, (b) rolled yellow sheet, (c) banana in ripening stage 6, (d) banana in ripening stage 1, and (e) red pepper.

Table 1
Experimental matrix and results of L^*, a^*, and b^* color scales for bananas

Experiment	Color_Back[a] (A)	Orientation degrees (B)	Resolution pixels (C)	Zoom[b] mm (D)	L^*	a^*	b^*
1	Black	0	640 × 480	5.4	71.3 ± 1.2	−1.0 ± 0.9	50.3 ± 1.2
2	White	0	640 × 480	5.4	79.9 ± 0.8	−1.3 ± 0.8	48.9 ± 1.7
3	Black	90	640 × 480	5.4	72.1 ± 1.6	−1.1 ± 0.9	50.5 ± 1.5
4	White	90	640 × 480	5.4	79.8 ± 1.1	−1.1 ± 0.9	49.1 ± 1.4
5	Black	0	2048 × 1536	5.4	71.6 ± 0.9	−0.4 ± 0.9	50.4 ± 1.4
6	White	0	2048 × 1536	5.4	80.6 ± 0.9	−0.7 ± 0.8	48.7 ± 1.5
7	Black	90	2048 × 1536	5.4	72.2 ± 1.2	−0.4 ± 0.9	50.5 ± 1.4
8	White	90	2048 × 1536	5.4	80.7 ± 0.9	−0.7 ± 0.9	48.8 ± 1.6
9	Black	0	640 × 480	11.3	72.3 ± 1.6	−1.1 ± 1.0	51.0 ± 1.5
10	White	0	640 × 480	11.3	80.7 ± 1.1	−1.4 ± 0.9	49.2 ± 1.5
11	Black	90	640 × 480	11.3	72.2 ± 1.5	−0.9 ± 0.9	50.7 ± 1.4
12	White	90	640 × 480	11.3	80.8 ± 1.1	−1.2 ± 0.9	49.1 ± 1.8
13	Black	0	2048 × 1536	11.3	72.5 ± 1.4	−0.4 ± 1.0	51.0 ± 1.6
14	White	0	2048 × 1536	11.3	81.0 ± 1.0	−0.4 ± 1.1	48.8 ± 1.5
15	Black	90	2048 × 1536	11.3	73.0 ± 1.0	−0.3 ± 0.9	50.6 ± 1.2
16	White	90	2048 × 1536	11.3	81.5 ± 1.1	−0.1 ± 0.9	48.1 ± 1.5
17 (CP)	Black	45	1024 × 768	7.8	71.4 ± 1.2	−0.4 ± 1.0	50.9 ± 1.4
18 (CP)	White	45	1024 × 768	7.8	80.1 ± 0.9	−1.1 ± 0.9	48.8 ± 1.4

[a] Color_Back represents the background color of the system.
[b] 5.4 mm represents the focal length without zoom.

For each color scale the cross-section profile was constructed using the average values of the pixels equidistant to the axis of the segmented image of the object. The lateral positions were coded as angular values varying from −90° to 90°, as shown for the rolled paper in Fig. 2. The color line profile was estimated from the smoothed pixel values for each color scale by using the function '*smooth*' which is implemented in Matlab and uses a 5-point moving average method. To avoid the borders in the yellow sheet as well as for non-homogeneous color regions in bananas (such as brown spots), the extremes of the segmented images were clipped at 5% for flat and rolled yellow sheets and at 15% for bananas as shown in Fig 1.

2.3. Statistical analysis

Statistical evaluations of the different experiments were performed by means of Statgraphics Plus for Windows software, Version 5.1 (Manugistic, Inc., Rockville, MD, USA).

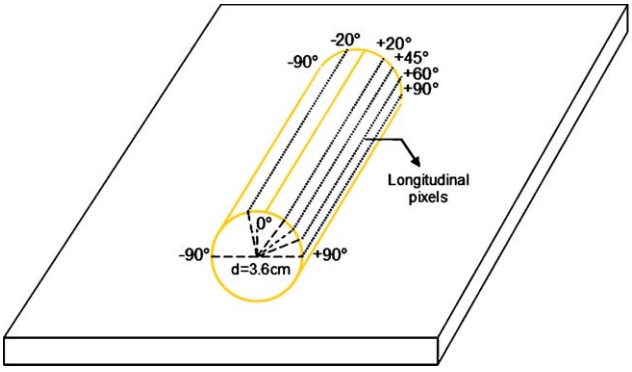

Fig. 2. Schematic representation of the color profile analysis for rolled yellow paper.

Applied methods were: simple regression analysis, analysis of variance for factorial experimental design with 95% confidence level.

3. Results and discussion

3.1. Calibration of the CVS: transformation of computer $R'G'B'$ into CIE XYZ space

Fig. 3a shows the plot of the $R'G'B'$ values acquired by CVS against their corresponding *RGB* values measured by colorimeter on the 125 Pantone® color sheets. The results clearly showed the nonlinear relationship among *RGB* values that is typical of many devices, meaning that the expected gamma correction needs to be applied to each of the tristimulus values of the CVS.

Fig. 3b shows that using the recommended IEC transfer functions (Eqs. (1)–(3)), which considered a gamma value equal to 2.4, a clear linear relationship is obtained with a reasonable fit between CIE *XYZ* values from the CVS and *XYZ* values from the colorimeter, giving variance accounted for R^2 higher than 0.97 for all the regression functions. Furthermore, the quantification of the $L^*a^*b^*$ color differences (Eq. (8)) among colorimeter and CVS revealed that the worst case corresponded to the cyan color hues with $\Delta E^*_{ab} = 12$.

The *sRGB* and CIE *XYZ* tristimulus values provide a CCD gamut characterization which can be used as an intermediate step for the transformation of any color image in other perceptual color spaces such as $L^*a^*b^*$ and *HSV*. Compatibility with the recommendations of the IEC 61966-2-1 and ITU-R BT.709 standards for color reproduction process that are typical of the Internet are maintained. Besides, the color information can be easily processed, duplicated, modified or transmitted via a network among industries or research lab-

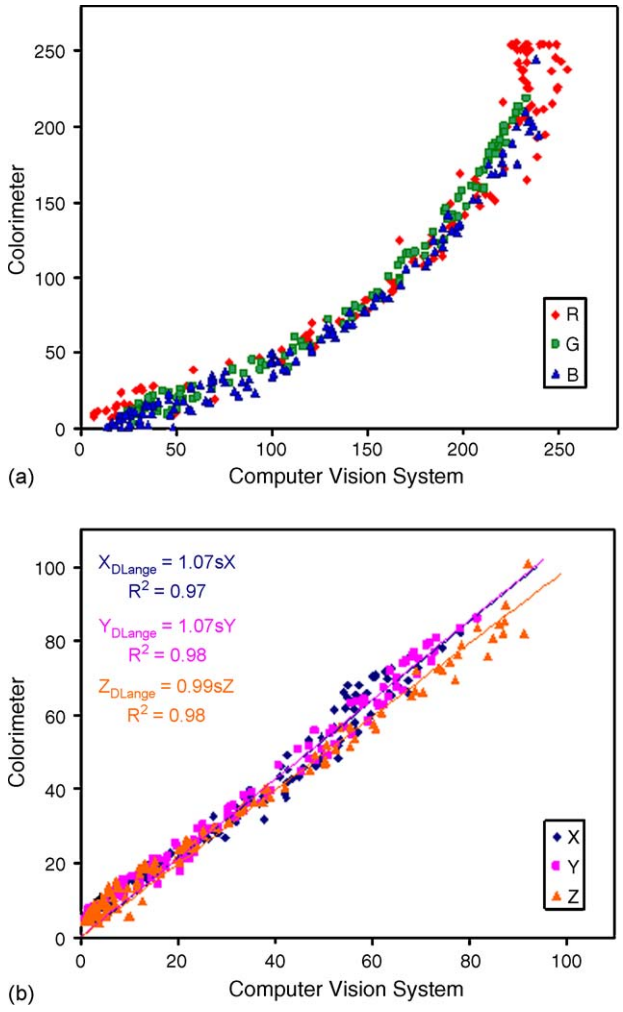

Fig. 3. Responses by CVS and colorimeter of the 125 Pantone® color sheets: (a) $R'G'B'$ values before to the transformation; (b) XYZ values after to the transformation.

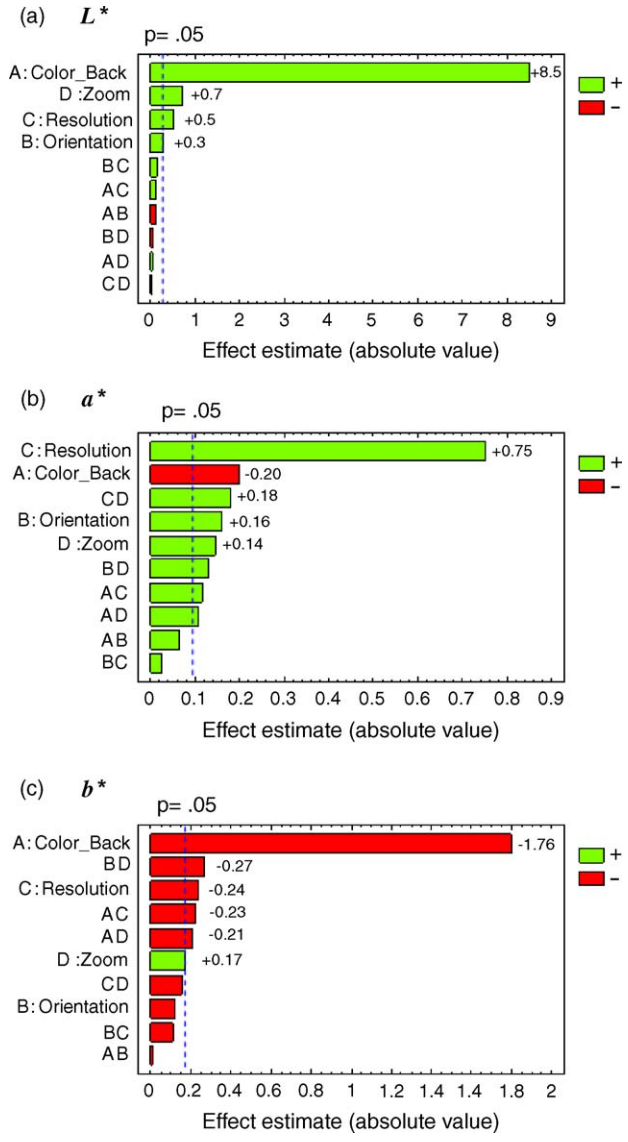

Fig. 4. Pareto charts of effects on the L^*, a^* and b^* bands for bananas in ripening stage 7 (yellow, flecked with brown spots). The vertical lines define the 95% confidence interval, and the values in the bars represent the absolute effect when the factor changes from low to high level.

oratories. Currently, *sRGB* is a representative color space for the majority of devices and color management systems on which color is captured and viewed. Therefore, its colorimetric definitions and mathematical transformations could also be extended for color measurement in CVSs implemented with video cameras or scanners.

It is important to state that color reproduction of the original scene is obtained in different calibrated computer monitors, even with applications where only color measurements are the final output. The modern food business is global and such visual communication link between growers, processors and traders at different parts of the world may facilitate optimal crop monitoring, product development, quality control and selection of food products.

3.2. Sensitivity of CVS for color measurements

Table 1 summarises the experimental design matrix, the average L^*, a^*, and b^* values and standard deviation derived from each run. Also, the results of central points (CP) for sample orientation (45°), resolution of CCD (1024×768) and focal length (7.8 mm) were included for comparison. Fig. 4 shows the Pareto charts of effects for each color scale based on the analysis of variance. Interpretation of the Pareto charts leads to the conclusion that among the factors and interactions statistically significant ($P < 0.05$), color of the background on L^* and b^* and resolution on a^* are the factors with the largest effects, as revealed by the absolute effects related to these color scales (Fig. 4a–c). When the color background was changed from black to white, L^* increased and b^* decreased in +8.5 and −1.8 units of color, respectively. The rest of factors and interactions in all color scales were characterized by smaller effects than one unit of color. In general, banana images looked lighter when the white background was used, than on the black background. This is because the white

background increases the light diffusivity in the system, and consequently, the light reflections from the sample detected by the CCD. The minimum L^* difference distinguishable by the human eye is about one unit (Poynton, 1996), and color differences in a^* and b^* for each unit of color represents color changes of 0.416%. The slight increases on a^* (+0.75) due to changes in the resolution may be caused by accuracy differences of the segmentation process. When the region of interest is extracted from the background, the segmentation is dependent on the color contrast between sample and background, and mainly on edge sharpness definition and shadows around of the edges. Therefore, slight errors in the segmentation process are more probable for images captured with lower resolution than those with the highest resolutions. Therefore, although statistically significant effects on L^*, a^* and b^* were obtained for other factors and interactions, in practical applications color measurements by CVS are mainly affected by the color of the background. Experimental results in the CP (Table 1) confirm the strong dependency of L^* values when the color of the background is changed from black to white and the moderated stability of the CVS to changes in other factors.

The compression of the image and resolution are considered the two major factors affecting the quality of the image (Russ, 2005). In this investigation all the images were stored in the JPEG compression format (which depends on discarding information that would not be perceived) because JPEG is the most popular algorithm used in many imaging devices and is now recognized as a standard for image exchanges. Furthermore, the time taken to process an image is directly related to both size and spatial resolution of the image, and this processing time is not frequently available in quality control and even in the labs. For color measurements of foods, images can be stored in JPEG format when the compression techniques preserve all the relevant and important image information needed to characterize the overall color surface. Nevertheless, in other applications such as in microscopy and image texture analysis, the quality of image may play a determinant role. For research purpose, Yam and Papadakis (2004) have recommended a CCD with a minimum resolution of 1600×1200 pixels and the use of non-compressed files such as TIFF format.

3.3. Effect of curved surfaces on color measurements

Since the *RGB*, $L^*a^*b^*$ and *HSV* color systems do not scale the information in the same way, each one can reflect variations in color not found by the other, the performance of these three color spaces could be analyzed to determine their suitability to quantify color in curved surfaces. Fig. 5 shows the color profile variation for the yellow sheet when it is flat and rolled using the normalized values for *sRGB* and $L^*a^*b^*$, and for *HSV* color space in the range 0–1. Examining the figures (Fig. 5a–c) it can be clearly seen that the color measurements are affected by the curvature of the surface, where the *sRGB* is the most affected among the three

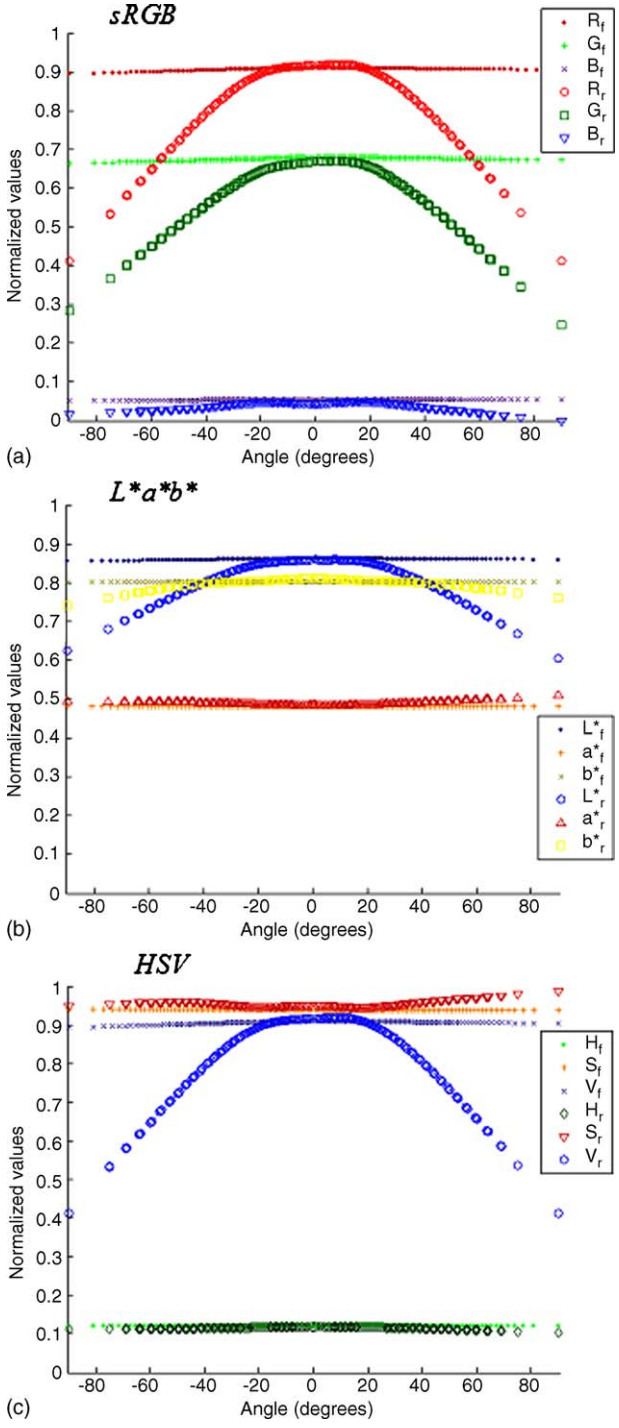

Fig. 5. Color profiles for the flat and rolled yellow sheet. (a) In *sR*, *sG*, *sB* scales, (b) in L^*, a^*, b^* scales, and (c) in *H*, *S*, *V* scales (subscripts f and r represent flat and rolled sheets).

compared color systems. Also, the L^* and *V* scales, which are measurements of the lightness, appear as the most affected by the curvature of the sample among the color scales of $L^*a^*b^*$ and *HSV* systems.

It should be clear from the previous sections that image acquisition of color is dependent on the surface reflectance

of the object and the intensity of the light source shining on it. In this context, for flat homogeneous color surfaces the directions and distribution of the reflected light intensities are expected to be homogeneous in any position of the sample, subsequently, giving constant color measurements anywhere. This fact has been confirmed in all analyzed range (from −90° to 90°) and for all color scales (Fig. 5a–c), demonstrating that both the yellow sheet and the light distribution were homogeneous for the CVS. The effect of light reflection is dependent on the position of the light source relative to the surface of the sample. The incident light from each opposite lamp (at 45° with the center of the background) could only illuminate with the same intensity, the frontal side of the cylinder closer to each lamp and part of their opposite side, making shadows around it. The extent of the shadows is dependent on the size, shape and degree of curvature of the sample. In addition for curved surfaces, the light reflections are affected by the extent of the radius of curvature of the surface which produces a complex arc of reflections and intensities that also vary along the surface of the sample. Thus, for the rolled sheet, symmetric color differences were mainly observed for the sR, sG, sB, L^* and V color scales when increasing the distance from the center to the edges of the cylinder. These color profiles were approximately constant in the range of −20° to 20° and similar to the average profiles obtained for the flat sheet. At higher angle modulus, the color profiles diminish continuously toward the lateral edges of the cylinder (−90° and 90°, respectively). Also, a slight disagreement in the constant range among the flat and rolled profiles for the sR, b^* and V scales was noticed, since the surface of rolled sheet was closer to the illuminants compared to the flat sheet, increasing slightly the registered intensity values.

The surface of fruit and vegetables are commonly curved and their topography may not be homogeneous. To determine the effect of these physical characteristics on the color and to confirm the best performance of $L^*a^*b^*$ and HSV in curved surfaces with different colors, the profiles for yellow and green bananas and red pepper were plotted in Fig. 6. For analysis, it could be assumed that the extended peel of each fruit, which visually presented a homogeneous color distribution, should approximately show a constant color profile for each color scale.

Although the shape of bananas is frequently characterized by the irregular polygonal surface of longitudinal planes (such as a polyhedron), for yellow and green bananas (Fig. 6a and b), similar profiles to those found for the rolled sheet were observed. The L^* and V color scales confirmed the high sensitivity to the curvature of the surface, as also was the S scale sensitive to the curvature of the bananas. For the a^*, b^* and H scales no color variations were observed.

For the red pepper (Fig. 6c), however, all color profiles showed the effect of undulations on the surface, the H scale being the most affected. The irregular undulations of the red pepper surface not only disturbed the directions and distribution of the reflected light intensities, but also produced shadows on the surface. Another factor contributing to the color variations is the glossiness of the surface, which enhances the contrast among the peaks and valleys of the undulations on the surface. The effect of gloss is clearly appreciated in the image of red pepper showed in Fig. 1e.

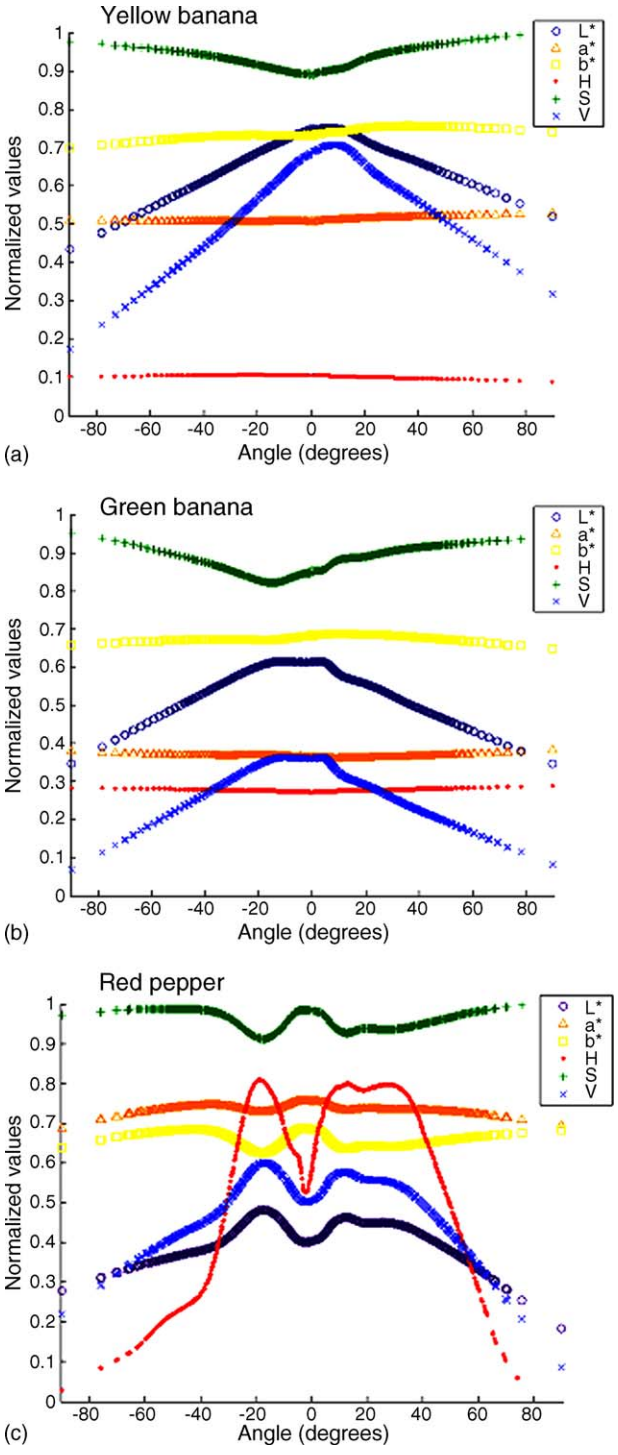

Fig. 6. Color profiles expressed in $L^*a^*b^*$ and HSV color scales for: (a) yellow banana; (b) green banana; and (c) red pepper.

These results revealed that the $L^*a^*b^*$ color system is more appropriate for color representation in surfaces or materials

with natural curvatures and undulations which are illuminated by a light source. In general, the registered light intensities using $L^*a^*b^*$ were less affected by shadows and areas of glossiness on the object surface. Therefore, among the three color systems evaluated, the $L^*a^*b^*$ system is recommended as the best space for color quantification in foods.

4. Conclusions

A de facto standard (*sRGB*) for the spectral sensitivities of practical recording devices adopted by the IEC 61966-2-1 (1999) was shown to be straightforward, efficient and simple to implement in Matlab. The correlation coefficients for *XYZ* values obtained from calibrated CVS and colorimeter for 125 color sheets showed good color matching with an $R^2 > 0.97$ in all regressions.

A sensitivity analysis of the implemented CVS using bananas demonstrated that the color measurements of lightness (L^* values) are significantly affected when the color of the background changed from the black to white. Also, color analysis in samples with curved surfaces reveled that the $L^*a^*b^*$ is more appropriate for color representation of surfaces or materials illuminated by a light source. These color profiles were less affected by the degree of curvature, shadows and glossiness of the surfaces than the *RGB* and *HSV* color systems, and therefore, more appropriate for color measurements of food surfaces. Finally, the CVS seems to be a good tool to quantify easily and quickly the color of any food using equipment that is readily available at reasonable cost. However, average color results from curved surfaces should be interpreted with caution.

Acknowledgments

Thanks to MECESUP/PUC 9903 Project (Chile) for granting the first author a doctoral scholarship at the School of Engineering, Pontificia Universidad Católica de Chile, and ALFA Programme (EC) – EU Alfa Project II-0121-FA for financial assistance to develop part of this investigation at Lund University.

Appendix A

CCD	*Charge Coupled Device*. Sensor for recording images, consisting of an array of linked or coupled capacitors which respond to red, green and blue lights
Gamma correction	A correction factor applied to linearize the relationship between screen luminance and electron gun voltage
HSV	An approximately uniform color space. It is defined directly as a nonlinear transformation of *RGB*
$L^*a^*b^*$	International standard for color measurement developed by CIE in 1976. Perceptually uniform and device-independent color space providing consistent color regardless of the input or output device (i.e. camera, scanner, monitor, and printer)
RGB	Universally accepted color system for color representation in television and video sets, CRT displays and many capture devices using red, green and blue primaries. It is not a perceptually uniform color space, i.e. differences between colors in the 3D *RGB* space do not correspond to color differences as perceived by humans
$R'G'B'$	Raw *RGB* data as produced by a digital camera or any capture device. The prime symbol represents the nonlinearity of their tristimulus values, and whose responses can differ on different digital cameras
sRGB	Device independent color model whose tristimulus values (*sR*, *sG*, *sB*) reproduce the same color on different devices, and represent linear combinations of the CIE *XYZ*. They are computed considering specific illumination conditions (D_{65}), a set of spectral sensitivities ($R'G'B'$) for a capture device, and a power function with a gamma value of 2.4, which closely fit a straightforward gamma 2.2 of standard CRT displays
XYZ	Device independent color system created by CIE in 1931. CIE *XYZ* is based on direct measurements of the human eye, and serves as the basis from which many other color spaces are defined

References

Abdullah, M.Z., Guan, L.C., Lim, K.C., Karim, A.A., 2001. The applications of computer vision system and tomographic radar imaging for assessing physical properties of food. J. Food Eng. 61, 125–135.

Brosnan, T., Sun, D.-W., 2002. Inspection and grading of agricultural and food products by computer vision systems—a review. Comput. Electron. Agric. 36, 193–213.

Brosnan, T., Sun, D.-W., 2004. Improving quality inspection of food products by computer vision—a review. J. Food Eng. 61, 3–16.

Castleman, K., 1996. Digital Image Processing. Prentice-Hall, Englewood Cliffs, NJ, 667 pp.

Chen, Y.-R., Chao, K., Kim, M.S., 2002. Machine vision technology for agriculture applications. Comput. Electron. Agric. 36, 173–191.

CIE, 1986. Colorimetry, Official recommendations of the International Commission on Illumination, CIE Publication No. 15.2. CIE Central Bureau, Vienna.

Du, C.-J., Sun, D.-W., 2004. Recent developments in the applications of image processing techniques for food quality evaluation. Trends Food Sci. Technol. 15, 230–249.

Du, C.-J., Sun, D.-W., 2005. Comparison of three methods for classification of pizza topping using different colour space transformations. J. Food Eng. 68, 277–287.

Francis, F.J., Clydesdale, F.M. (Eds.), 1975. Food Colorimetry: Theory and Applications. AVI Publishing Co., Westport, CT, 477 pp.

Gondek, J. 2000. An extended sRGB space for high quality consumer imaging. Revision 1.01 6/20/00. Hewlett-Packard.

Hunt, R.W.G. (Ed.), 1991. Measuring of Colour. Ellis Horwood, Ltd., New York, p. 313.

Hunter, R.S., Harold, R.W. (Eds.), 1987. The Measurement of Appearance. John Wiley & Sons, New York, 411 pp.

Hutchings, J.B. (Ed.), 1999. Food Color and Appearance. Aspen Publishers, Inc., Gaithersburg, MD, p. 593.

Hutchings, J.B., Luo, R., Ji, W., 2002. Calibrated colour imaging analysis of food. In: MacDougall, D. (Ed.), Colour in Food. Woodhead Publishing, pp. 352–366 (Chapter 14).

IEC 61966-2-1, 1999. Multimedia systems and equipment – Colour measurements and management – Part 2-1: Colour management – Default RGB color space – sRGB' (International Electrotechnical Commission, Geneva, 1999-10).

Mendoza, F., Aguilera, J.M., 2004. Application of image analysis for classification of ripening bananas. J. Food Sci. 69, 471–477.

O'Sullivan, M.G., Byrne, D.V., Martens, H., Gidskehaug, L.H., Andersen, H.J., Martens, M., 2003. Evaluation of pork color: prediction of visual sensory quality of meat from instrumental and computer vision methods of color analysis. Meat Sci. 65, 909–918.

Papadakis, S., Abdul-Malek, S., Kamdem, R.E., Jam, K.L., 2000. A versatile and inexpensive technique for measuring color of foods. Food Technol. 54, 48–51.

Poynton, C. (Ed.), 1996. A Technical Introduction to Digital Video. John Wiley & Sons, New York, pp. 91–114 (Chapter 6: Gamma).

Robertson, A.L., 1976. The CIE 1976 color difference formulae. Color Res. Appl. 2, 7–11.

Rec. ITU-R BT.709-5, 2002. Parameter values for the HDTV standards for production and international programme exchange (1990, revised 2002). International Telecommunication Union, 1211 Geneva 20, Switzerland.

Russ, J.C. (Ed.), 2005. Image Analysis of Food Microstructure. CRC Press LLC, New York, 369 pp.

Sangwine, S.J., 2000. Colour in image processing. Electron. Commun. Eng. J. 12, 211–219.

Segnini, S., Dejmek, P., Öste, R., 1999. A low cost video technique for color measurement of potato chips. Lebensm.-Wiss. U.-Technol. 32, 216–222.

Shahin, M.A., Symons, S.J., 2001. A machine vision system for grading lentils. Can. Biosyst. Eng. 43, 7.7–7.14.

Stokes, M., Anderson, M., Chandrasekar, S., Motta, R., 1996. A standard default color space for the internet—sRGB, Version 1.10. International Color Consortium (ICC), 1899 Preston White Drive, Reston, VA, November 5.

Yam, K.L., Papadakis, S.E., 2004. A simple digital imaging method for measuring and analyzing color of food surfaces. J. Food Eng. 61, 137–142.